AD-A126 070 SEM (SCANNING-ELECTRON-MICROSCOPY) STUDIES OF MAGNETIC DOMAINS IN AMORPHO..(U) GENERAL ELECTRIC CORPORATE RESEARCH AND DEVELOPMENT SCHENECTA.. J D LIVINGSTON 1/1

UNCLASSIFIED 31 JAN 83 83-SRD-013 N00014-82-C-0060 F/G 11/6 NL

END

FILMED

DTIC

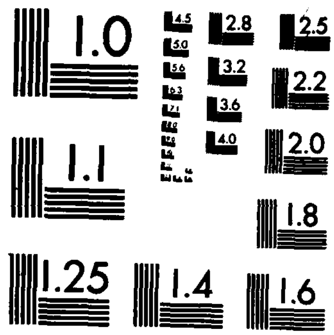

MICROCOPY RESOLUTION TEST CHART
NATIONAL BUREAU OF STANDARDS-1963-A

AD A126070

SEM STUDIES OF MAGNETIC DOMAINS IN AMORPHOUS METALS

Annual Report
Contract No. N00014-82-C-0060

Prepared for

Department of the Navy
Office of Naval Research
Arlington, Virginia 22217

Prepared by

Properties Branch
Metallurgy Laboratory
Corporate Research and Development
General Electric Company
Schenectady, New York 12301

January 1983

83-SRD-013

unclassified

SECURITY CLASSIFICATION OF THIS PAGE (When Data Entered)

REPORT DOCUMENTATION PAGE

READ INSTRUCTIONS BEFORE COMPLETING FORM

1. REPORT NUMBER	2. GOVT ACCESSION NO. AD-A126070
3. RECIPIENT'S CATALOG NUMBER	
4. TITLE (and Subtitle) SEM Studies of Magnetic Domains in Amorphous Metals	5. TYPE OF REPORT & PERIOD COVERED Annual Report 1 Dec 1981- 30 Nov 1982
	6. PERFORMING ORG. REPORT NUMBER 83-SRD-013
7. AUTHOR(s) J. D. Livingston	8. CONTRACT OR GRANT NUMBER(s) N00014-82-C-0060
9. PERFORMING ORGANIZATION NAME AND ADDRESS General Electric Company Corporate Research and Development Schenectady, NY 12301	10. PROGRAM ELEMENT, PROJECT, TASK AREA & WORK UNIT NUMBERS
11. CONTROLLING OFFICE NAME AND ADDRESS Department of the Navy Office of Naval Research Arlington, VA 22217	12. REPORT DATE 31 January 1983
	13. NUMBER OF PAGES 21
14. MONITORING AGENCY NAME & ADDRESS (if different from Controlling Office)	15. SECURITY CLASS. (of this report) unclassified
	15a. DECLASSIFICATION/DOWNGRADING SCHEDULE

16. DISTRIBUTION STATEMENT (of this Report)

Approved for public release; distribution unlimited.

17. DISTRIBUTION STATEMENT (of the abstract entered in Block 20, if different from Report)

18. SUPPLEMENTARY NOTES

19. KEY WORDS (Continue on reverse side if necessary and identify by block number)

amorphous metals, magnetic domains, scanning electron microscopy, magnetic properties, magnetomechanical properties, magnetic anisotropy

20. ABSTRACT (Continue on reverse side if necessary and identify by block number)

Magnetic domain structures in transverse-annealed amorphous ribbons were characterized by SEM. Effects of ribbon width, anisotropy constant, ac and dc magnetic fields, and applied fields were demonstrated. Results were related to magnetic and magnetomechanical properties.

DD FORM 1 JAN 73 1473 EDITION OF 1 NOV 65 IS OBSOLETE

unclassified

SECURITY CLASSIFICATION OF THIS PAGE (When Data Entered)

TABLE OF CONTENTS

SEM STUDIES OF MAGNETIC DOMAINS IN AMORPHOUS METALS

Section 1 BACKGROUND

A. Amorphous Metals

Melt-spun ribbons of amorphous magnetic alloys, particularly alloys of transition metals such as Fe, Ni, and Co with metalloids such as B, Si, and C, have been under intensive study for several years. Their lack of grain structure and of magneto-crystalline anisotropy allows the attainment of excellent soft magnetic properties. In addition, they exhibit high mechanical strength and hardness and, in some cases, high corrosion resistance. As a result, these newly-available materials are being evaluated for various magnetic and magnetomechanical applications. Although their largest-volume application may eventually be as core materials in distribution transformers, in the near future they appear likely to be used primarily in high-frequency and electronic applications and as transducers and sensors, e.g., sonar sensors for the Navy.

An important feature of amorphous magnetic alloys, not yet fully exploited, is that their technical magnetic properties can be varied over a wide range by variations in annealing and processing history. These variations produce different distributions of magnetic anisotropies and magnetic domain structures, resulting in variations in ac losses, permeability, coercivity, magnetostriction, etc. Magnetic domain structures are determined largely by the specimen shape and by the orientation, symmetry, and magnitude of the magnetic anisotropies present. In amorphous metals, these anisotropies usually result from magnetic annealing and/or from internal or applied stresses interacting with magnetostriction.

B. Anisotropy Types

For 60-Hz transformer applications, ribbons have usually been annealed in a longitudinal field to produce <u>longitudinal</u> anisotropy, i.e., a low-energy or "easy" magnetic axis along the ribbon length. This can produce high permeabilities, low coercivities, and square-loop magnetic behavior. Magnetization in longitudinal field occurs primarily by the motion of 180° domain walls. Eddy-current losses are proportional to the average domain width, which can be 1 mm or more, and may be nearly 100 times higher than classically-calculated eddy-current losses.

Transverse anisotropy, i.e., an easy axis parallel to the ribbon width, produces maximum magnetomechanical coupling and is therefore of interest for transducer and sensor applications. Magnetization in longitudinal field occurs primarily by rotation rather than by domain-wall motion. Eddy-current losses are low, approaching the classical limit, and hence transverse anisotropy is also of interest for high-frequency applications. However, magnetostrictive length change is maximum, and the magnetic hysteresis loop is sheared, i.e., permeability is lowered.

Perpendicular anisotropy, with the easy axis normal to the ribbon plane, produces a very fine internal domain structure and a closure-domain structure at the surfaces. Magnetization in longitudinal fields will generally involve both rotation and domain-wall motion, yielding intermediate properties.

Easy-axis orientations between these three limiting cases, or oblique anisotropies, can also be produced. The resulting combination of properties may be favorable for particular applications.

C. Pre-Contract Work

Prior to the present contract, we had studied domain structures in amorphous metals by Bitter and scanning-electron-microscopy (SEM) techniques (1-6), in support of the General Electric development program for amorphous metal distribution transformers. Emphasis had been on ribbons with longitudinal anisotropy, although oblique in-plane anisotropy was also studied (5).

We proposed in August 1981 to use our techniques to study anisotropy and domain control in amorphous metals. Special emphasis was placed on transverse and oblique anisotropies because of their importance in transducer and high-frequency applications. Domain observations were to be coupled with magnetomechanical measurements by A. E. Clark and co-workers at the Naval Surface Weapons Center (NSWC).

In preparation for the contract, a simplified model of the magnetomechanical properties of transverse-anisotropy ribbons was developed (7). (Appendix A) The treatment emphasizes the importance of a low and uniform anisotropy in producing high magnetomechanical coupling, and is similar to that independently developed by Spano et al. (8). Plans for specific domain experiments were developed after a visit to NSWC in November 1981.

Section 2
CONTRACT PROGRESS

The major results to date were reported at the 1982 Intermag Conference in Montreal in July (9). (Appendix B) Samples studied included GE-prepared samples and transverse-annealed ribbons from NSWC with known magnetomechanical properties.

A. Equipment

Domain contrast in the SEM depends on the angle between the electron velocity and the magnetization vector. The sample holder used in previous studies provided optimum contrast for longitudinal-anisotropy ribbons, but contrast was low for transverse anisotropy. A new sample stage was developed that permits both rotation and tilting of the sample to achieve optimum domain contrast for various orientations of the magnetization. After slight modifications indicated by initial experiments, this new sample stage produced excellent domain contrast in transverse-anisotropy ribbons, as can be seen from Figs. 1-3 of Appendix B.

B. Effects of Ribbon Geometry

Domain widths in transverse-anisotropy ribbons were found to be of the order of 100 μm, about an order of magnitude narrower than in longitudinal-anisotropy ribbons. Zero-field domain widths are finer in narrow ribbons than in wide ribbons (Fig. 1a and b, Appendix B), and appear to be only slightly sensitive to magnetic history.

These various results indicate that domain widths in transverse-anisotropy ribbons are governed largely by energetic considerations. The energy of the domain walls themselves favors coarse domains, but the magnetostatic energy associated with transverse demagnetizing fields favors fine domains. Narrower (or thicker) ribbons have a larger transverse demagnetizing factor and therefore the energy balance tips towards finer domains.

C. Effects of Anisotropy Constant

Conclusions here were reached by comparisons of transverse-anisotropy ribbons of Allied 2605SC ($Fe_{81}B_{13.5}Si_{3.5}C_2$) and 2605CO ($Fe_{67}Co_{18}B_{14}Si_1$). Magnetic measurements made on these ribbons at NSWC indicated that the magnetic anisotropy constant in these CO ribbons was more than an order of magnitude higher than in the SC ribbons.

Domains in the CO ribbons were generally straighter than in the SC ribbons, in which domain curvature from residual or unintentional applied stresses and from edge demagnetizing fields was often severe (Figs. 2 and 3, Appendix B). The higher anisotropy of the CO ribbons apparently ties the magnetization more rigidly to the transverse direction, more closely approaching the idealized models of References 7 and 8. This important result is one reason why the properties of low-anisotropy alloys like SC depart from theoretical predictions.

Another interesting result was that domains were generally finer in CO ribbons (Fig. 1, Appendix B) than in SC ribbons (Fig. 2, Appendix B). This is contrary to expectations based on domain-wall energy alone, and results from the effect of anisotropy constant on the transverse demagnetizing energy through the μ^*-effect. According to classical domain theory, demagnetizing fields will lead to a rotation of the magnetization away from the easy direction. The susceptibility to this rotation, μ^*, varies as K^{-1}, and becomes dominant in the energy balance in low-anisotropy materials. As noted earlier, magnetomechanical coupling will be affected.

D. Effects of Applied Field

Application of a dc longitudinal field to transverse-anisotropy ribbons led to decreased domain contrast. This results from magnetization rotation towards the field direction, since it is the opposite components of transverse magnetization that produce the contrast.

More unexpectedly, the dc longitudinal field also led to a domain refinement (Fig. 1c, Appendix B). Review of the literature revealed that domain refinement by hard-axis magnetization had also been observed in some crystalline materials, and may be associated with the gradual transition from Bloch to Neel walls expected in this field orientation.

E. Effects of Applied Stress

Application of longitudinal tensile stresses to ribbons with transverse or in-plane oblique anisotropy produced rotation of the domains (Fig. 4, Appendix B). Measurement of the rotation angle with stress was used to determine the ratio K/λ_s, where K is the anisotropy constant and λ_s is the saturation magnetization.

In agreement with theory, domain rotation with stress was found to be much more abrupt with transverse anisotropy than with oblique anisotropy. Detailed analysis of this effect reveals the sensitivity of magnetomechanical coupling to slight deviations of the anisotropy K from the transverse direction.

F. Work to be Continued

Several other experiments have shown promising results and will be continued in an extension of this contract.

We have examined domain structures in alloys heat-treated to produce optimum high-frequency properties, in particular low eddy-current losses. Results to date indicate transverse or perpendicular anisotropies, probably resulting from internal stresses produced by partial crystallization.

We have annealed several samples in fields with a large component normal to the ribbon plane, in the hope of producing an out-of-plane oblique anisotropy. Such an anisotropy produces low eddy-current losses in silicon iron through domain refinement, and a similar effect in amorphous metals would be of interest. Significant domain refinement has been observed in some samples, but concurrent domain alignment and improved properties have not yet been achieved.

The effect of anisotropy constant on equilibrium domain widths is being studied quantitatively in transverse-annealed ribbons of $Co_{70.3}Fe_{4.7}Si_{15}B_{10}$. This zero-magnetostriction alloy was chosen for study because the kinetics of the development and reorientation of the induced anisotropy had previously been documented in detail by workers at the University of Pennsylvania. Samples of various anisotropy levels have been received from Dr. T. Jagielinski, and domain widths and behavior have been characterized. Changes in domain width with time have been observed at the lowest anisotropy levels. This work will be presented at the 1983 Intermag Conference in Philadelphia. The abstract submitted has been included as Appendix C.

Section 3

REFERENCES

1. "Stresses and Magnetic Domains in Amorphous Metal Ribbons", J.D. Livingston, Phys. Stat. Sol. (a) 56, 637 (1979).

2. "Cast-In Crystals in Amorphous Ribbons", J.L. Walter, J.D. Livingston and A.M. Davis, Mater. Sci. Eng. 49, 47 (1981).

3. "SEM Studies of Magnetic Domains in Amorphous Ribbons", J.D. Livingston and W.G. Morris, IEEE Trans. Magn. MAG-17, 2624 (1981).

4. "The Deleterious Effect of Aluminum in Fe-B-Si-C Amorphous Ribbon", H.C. Fiedler, J.D. Livingston and S.C. Huang, J. Magn. Magn. Mater. 26, 157 (1982).

5. "Effect of Annealing Angle on the Magnetic Properties of an Amorphous Fe-B-Si-C Alloy", F.E. Luborsky and J.D. Livingston, IEEE Trans. Magn. MAG-18, 908 (1982).

6. "Effects of Ribbon Thickness and Annealing Temperature on the AC Magnetic Properties of the $Fe_{81.5}B_{14.5}Si_3C_1$ Alloy", S.C. Huang, P.G. Frischmann, F.E. Luborsky, J.D. Livingston and A. Mogro-Campero, Proc. Symp. Rapidly-Solidified Amorphous and Crystalline Alloys, Materials Research Society (to be published).

7. "Magnetomechanical Properties of Amorphous Metals", J.D. Livingston, Phys. Stat. Sol. (a) 70, 591 (1982).

8. "Magnetostriction and Magnetic Anisotropy of Field Annealed Metglas 2605 alloys via dc M-H Loop Measurements Under Stress", M.L. Spano, K.B. Hathaway, and H.T. Savage, J. Appl. Phys. 53, 2667 (1982).

9. "Domain Studies on Amorphous Ribbons with Transverse or Oblique Magnetic Anisotropy", J.D. Livingston, W.G. Morris and F.E. Luborsky, 1982 Intermag Conference, J. Appl. Phys, 53, 7837 (1982).

10. "Kinetics of Formation of Induced Magnetic Anisotropy in a Zero-Magnetostriction Amorphous Alloy", K-Y Ho, P.J. Flanders, and C.D. Graham, Jr., J. Appl. Phys. 53, 2279 (1982).

11. "Theory and Application of Highly Magnetoelastic Metglas 2605SC", H.T. Savage and M.L. Spano, 1982 Intermag Conference, J. Appl. Phys. 53, 8092 (1982).

12. "Neel Walls in a Massive Uniaxial Ferromagnetic in an External Field", R. Gemperle and M. Zeleny, Phys. Stat. Sol. 6, 839 (1964).

13. "The Influence of Magnetostriction on the Magnetic Domain Structure of Uniaxial Crystals, Cobalt in Particular", A. Hubert, Phys. Stat. Sol. 22, 709 (1967).

APPENDIX A:

"MAGNETOMECHANICAL PROPERTIES OF AMORPHOUS METALS"

APPENDIX B:

"DOMAIN STUDIES ON AMORHOUS RIBBONS WITH
TRANSVERSE OR OBLIQUE MAGNETIC ANISOTROPY"

APPENDIX C:

"EFFECTS OF ANISOTROPY ON DOMAIN
STRUCTURES IN AMORPHOUS RIBBONS" (abstract)

APPENDIX A

phys. stat. sol. (a) 70, 591 (1982)

Subject classification: 12.1 and 18.2; 2; 21

Metallurgy Laboratory, General Electric Corporate Research and Development, Schenectady[1])

Magnetomechanical Properties of Amorphous Metals

By

J. D. LIVINGSTON

Amorphous metals have magnetomechanical properties superior to those of crystalline magnetostrictive materials, and are therefore being considered for a variety of transducer and sensor applications. A simplified model is presented of magnetomechanical coupling in amorphous metal ribbons, showing the relation between magnetomechanical behavior and fundamental material parameters. Although high values of magnetization and magnetostriction are important, it is primarily the low values of magnetic anisotropy achievable that give amorphous metals their outstanding magnetomechanical coupling. The magnitude and homogeneity of this anisotropy is controllable through choice of alloy composition and annealing conditions.

Amorphe Metalle haben bessere magnetomechanische Eigenschaften als kristalline Werkstoffe, und werden deshalb für Anwendungen als Energieumwandler und Kraftübertrager betrachtet. Ein vereinfachtes Modell der magnetomechanischen Kopplung in amorphen metallischen Bändern wird gegeben, das die Beziehung zwischen magnetomechanischem Verhalten und grundlegenden Parametern des Werkstoffes erklärt. Obwohl hohe Werte der Magnetisierung und Magnetostriktion wichtig sind, stammen die hervorragenden magnetomechanischen Kopplungseigenschaften in amorphen Metallen hauptsächlich von den niedrigen Werten der magnetischen Anisotropie. Die Werte und die Homogenität der Anisotropie werden durch die Legierungszusammensetzung und die Anlaßbedingungen kontrolliert.

1. Introduction

Amorphous metals have been shown to have magnetomechanical properties superior to those of any previous magnetic materials [1 to 5]. As a result, they are being considered for a variety of transducer and sensor applications. As a guide to understanding, optimizing, and applying these properties, we present here a simplified model of magnetomechanical coupling in amorphous metal ribbons.

In amorphous metals, the major sources of magnetic anisotropy are structural anisotropies induced by annealing under magnetic field (and/or applied stress) and magnetostrictive anisotropies produced by the interaction between magnetostrictive strain and applied or residual stresses. Magnetomechanical properties are determined by the competition between these two sources of anisotropy.

2. Model

We consider an amorphous metal ribbon annealed in a large magnetic field parallel to the ribbon width to produce a widthwise magnetic easy axis. We assume a first-order uniaxial anisotropy, with an energy contribution of $K_u \cos^2 \theta$ per unit volume, where $K_u > 0$ and θ is the angle between the magnetization (assumed to remain in the ribbon plane) and the ribbon length. With zero applied field and zero applied stress, the resulting domain structure will be as shown in Fig. 1a. A longitudinal

[1]) P.O.B. 8, Schenectady, New York 12301, USA.

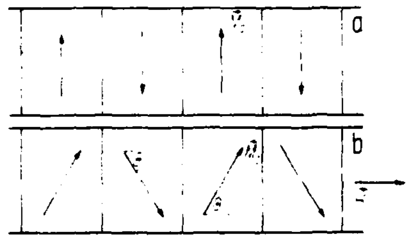

Fig. 1. a) Zero-field domain structure of transverse-annealed amorphous ribbon. b) Domain structure of transverse-annealed ribbon in longitudinal magnetic field $H < H_A$

magnetic field H will rotate the magnetization from the width towards the length direction (Fig. 1b) and make a contribution to the energy density of $-M_sH\cos\theta$ where M_s is the domain magnetization per unit volume. Finding the angle θ for minimum energy yields for the longitudinal component of magnetization

$$M = M_s \cos\theta = M_s \frac{H}{H_A} \qquad (H \leqq H_A)\,, \tag{1}$$

where $H_A = 2K_u/M_s$ is the anisotropy field. The susceptiblity is constant for $H < H_A$ and equal to

$$\chi \equiv \frac{dM}{dH} = \frac{M_s}{H_A} = \frac{M_s^2}{2K_u}. \tag{2}$$

The spontaneous magnetostrictive strain in each domain is λ_s in the direction of magnetization and $-\lambda_s/2$ in orthogonal directions. Thus, as the magnetization rotates from the width to the length direction, the longitudinal strain ε changes from $-\lambda_s/2$ to $+\lambda_s$, a change of $3\lambda_s/2$. As a function of θ, and, through equation (1), as a function of H, the longitudinal strain is given by

$$\varepsilon = \frac{3\lambda_s}{2}\left(\cos^2\theta - \frac{1}{3}\right) = \frac{3\lambda_s}{2}\left(\frac{H^2}{H_A^2} - \frac{1}{3}\right). \tag{3}$$

Hence

$$d \equiv \frac{d\varepsilon}{dH} = \frac{3\lambda_s H}{H_A^2}. \tag{4}$$

This measure of magnetomechanical coupling reaches a maximum at $H = H_A$,

$$d_{max} = \frac{3\lambda_s}{H_A} = \frac{3\lambda_s M_s}{2K_u}. \tag{5}$$

We now consider the application of a longitudinal stress σ, which produces an anisotropic contribution to the energy density of $-\frac{3}{2}\lambda_s\sigma\cos^2\theta$ [6]. Thus the net anisotropy energy will now be $(K_u - \frac{3}{2}\lambda_s\sigma)\cos^2\theta$. For $\lambda_s\sigma > 0$, i.e. tensile stress on a positive-magnetostriction material or compressive stress on a negative-magnetostriction material, the stress has the effect of lowering the net anisotropy from K_u to $(K_u - \frac{3}{2}\lambda\sigma)$. The magnetic easy axis will remain in the width direction as long as $\sigma < \sigma_c = 2K_u/3\lambda_s$, but will abruptly switch to the length direction for $\sigma > \sigma_c$. We will consider only the former case.

Magnetization behavior will be as before with H_A replaced by a reduced anisotropy field

$$H_{A\sigma} \equiv \frac{2K_u - 3\lambda_s\sigma}{M_s} \qquad (\sigma \leqq \sigma_c)\,. \tag{6}$$

Thus

$$M = M_s \frac{H}{H_{A\sigma}} \qquad (H \leqq H_{A\sigma}), \tag{7}$$

$$\chi_\sigma \equiv \left(\frac{\partial M}{\partial H}\right)_\sigma = \frac{M_s}{H_{A\sigma}}, \tag{8}$$

$$d \equiv \left(\frac{\partial M}{\partial \sigma}\right)_H = \frac{3\lambda_s H}{H_{A\sigma}^2}. \tag{9}$$

This dependence of M on H and σ is shown graphically in Fig. 2a and b.

The magnetostrictive contribution to longitudinal strain ε will be given by (3) with H_A replaced by $H_{A\sigma}$. There will in addition be a Hooke's law term σ/E_M, where E_M is the Young's modulus at constant magnetization (for example, at saturation). Thus

$$\varepsilon = \frac{\sigma}{E_M} + \frac{3\lambda_s}{2}\left(\frac{H^2}{H_{A\sigma}^2} - \frac{1}{3}\right), \tag{10}$$

$$d \equiv \left(\frac{\partial \varepsilon}{\partial H}\right)_\sigma = \frac{3\lambda_s H}{H_{A\sigma}^2}, \tag{11}$$

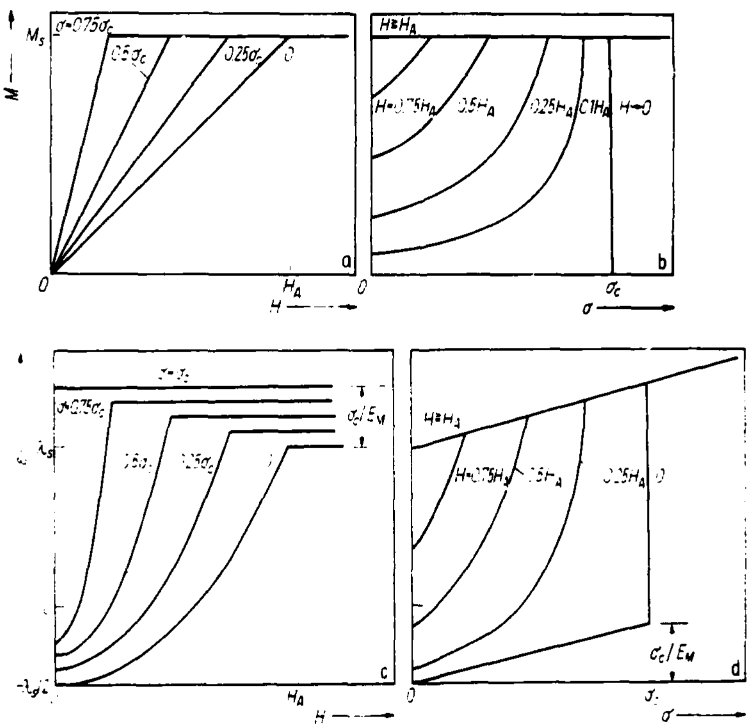

Fig. 2. Results of idealized model. a) Variation of longitudinal magnetization M with longitudinal field H at various values of longitudinal stress σ. b) Variation of M with σ at various values of H. c) Variation of longitudinal strain ε with H at various values of σ. d) Variation of ε with σ for various values of H. In real materials, inhomogeneities in anisotropy and other parameters will lead to rounded, instead of sharp, transitions

$$\frac{1}{E_H} = \left(\frac{\partial\varepsilon}{\partial\sigma}\right)_H = \frac{1}{E_M} + \frac{9\lambda_s^2 H^2}{M_s H_{A\sigma}^3}. \tag{12}$$

This dependence of ε on H and σ is shown graphically in Fig. 2c and d.

A parameter of direct importance in transducer and sensor applications is $d = (\partial\varepsilon/\partial H)_\sigma = (\partial M/\partial\sigma)_H$, the so-called piezomagnetic strain constant. (These two partial derivatives are equal through Maxwell's relations.) This quantity reaches a maximum value at $H = H_{A\sigma}$ of

$$d_{max} = \frac{3\lambda_s}{H_{A\sigma}} = \frac{3\lambda_s M_s}{2K_u - 3\lambda_s\sigma}. \tag{13}$$

Another important parameter for comparing materials is the magnetomechanical coupling factor k, which is related to the fractional energy transfer between magnetic and mechanical energy, and thus is a basic index of energy conversion capability [7, 8]. It can be related [7] to the parameters already derived, and equals

$$k = d\left(\frac{E_H}{\chi_\sigma}\right)^{1/2} = \left[1 + \frac{M_s H_{A\sigma}^3}{9\lambda_s^2 E_M H^2}\right]^{-1/2} \leqq 1 \tag{14}$$

which reaches, at $H = H_{A\sigma}$, a maximum value of

$$k_{max} = \left[1 + \frac{2K_u - 3\lambda_s\sigma}{9\lambda_s^2 E_M}\right]^{-1/2} \leqq 1. \tag{15}$$

For applications based on changes in elastic modulus, the parameter of interest is the fractional difference between the elastic modulus at constant magnetization and the modulus at constant field. From (12),

$$\frac{\Delta E}{E_H} \equiv \frac{E_M - E_H}{E_H} = \frac{9\lambda_s^2 E_M H^2}{M_s H_{A\sigma}^3} \tag{16}$$

reaching a maximum at $H = H_{A\sigma}$ of

$$\left(\frac{\Delta H}{E_H}\right)_{max} = \frac{9\lambda_s^2 E_M}{2K_u - 3\lambda_s\sigma}. \tag{17}$$

3. Discussion

It is clear from (13), (15), and (17) why some Fe-rich amorphous ribbons have superior magnetomechanical properties. For an unstressed sample, d_{max} depends on $\lambda_s M_s/K_u$, and k_{max} and $(\Delta E/E_H)_{max}$ depend on $\lambda_s^2 E_M/K_u$. Fe-rich amorphous alloys can have substantial magnetostriction constants ($\lambda_s = (25 \text{ to } 50) \times 10^{-6}$) and, more importantly, can have very low anisotropies. For example, Allied 2605SC ($Fe_{81}B_{13.5}Si_{3.5}C_2$) has been annealed to produce $K_u = 38\ J/m^3$, $H_A = 70$ A/m (0.9 Oe), and $\sigma_c = 0.7$ MPa (100 psi) [5]. *It is these low values of K_u, H_A, and σ_c that permit rotation of the magnetization and accompanying magnetostrictive strain with low applied fields or stresses, yielding outstanding magnetomechanical properties.*

For 2605SC a coupling constant k of 0.98 and a $\Delta E/E_H$ exceeding ten have been estimated [5]. Most crystalline magnetostrictive materials have k-values of 0.3 or lower and $\Delta E/E_H$ less than unity. Even the rare-earth–iron compounds with giant magnetostriction constants, which are currently being considered for sonar applications, have only $k \approx 0.7$ (competitive with piezoceramic materials such as lead titanate zirconate) [8, 9].

The equations also show that the application of a longitudinal stress σ can further reduce the effective anisotropy and increase the magnetomechanical coupling. The maximum values given by (13), (15), and (17), however, are only achieved at a precise balance of field, stress, and anisotropy given by $H = H_{A\sigma}$. Further, in many applications it may not be desirable to further increase magnetomechanical coupling. Allied 2605SC may already be too sensitive for some applications.

This simplified model has assumed that K_u, λ_s, M_s, E_M, H, and σ are all completely homogeneous throughout the sample. In reality, there are likely to be inhomogeneities in all these quantities (leading, for example, to rounding of the "knee" of the magnetization curve [5]). Surface defects and irregularities will lead to local variations in σ, as will any components of bending or twisting. The non-ellipsoidal shape of the sample leads to variations in H. More importantly, the material parameters will be inhomogeneous, particularly K_u. A major source of variations in K_u will be internal stresses, which will lead to variations in both the amplitude and the direction of the net anisotropy. It is thus necessary that the anneal be sufficient to remove the internal stresses present in the as-cast ribbon without inducing significant crystallization. This may be difficult in alloy compositions with low crystallization temperatures.

Spano et al. [5] have observed in 2605SC the linear decrease of χ_σ^{-1} with σ predicted by (8), but found a minimum χ_σ^{-1} in excess of that expected from the demagnetizing factor alone. This minimum may result from the inhomogeneity in anisotropy, δK_u, which prevents $H_{A\sigma}$ from reaching zero simultaneously at all points in the sample. If this is the source of the observed minimum χ_σ^{-1}, we conclude $\delta K_u \approx 0.27 K_u \approx$ $\approx 10\ \mathrm{J/m^3}$. If this δK_u results from internal stresses, their magnitude is $\delta\sigma \approx 0.2$ MPa (30 psi). The presence of internal stresses of this magnitude in an annealed sample is not unreasonable. The δK_u value so estimated can also be used in (13), (15), and (17) to estimate the upper limits of the various magnetomechanical parameters obtainable by stressing.

The properties desired for high magnetomechanical sensitivity are high λ_s, M_s, and E_M, and low (and homogeneous) K_u. All these quantities vary with alloy composition. In particular, the induced anisotropy constant K_u of Fe-base amorphous alloys is increased strongly by the presence of additional transition elements such as Ni or Co [10, 11]. This is probably why the coupling factors of Allied 2605CO ($Fe_{67}Co_{18}B_{14}Si_1$) were inferior to those of 2605SC [1].

The value of K_u is also sensitive to annealing temperature and time, the kinetics of K_u development, and relief of quenched-in stresses both increasing with increasing temperature, but the ultimate value of K_u decreasing as the Curie temperature is approached [10 to 12]. In many alloys, a simple transverse-field anneal may not be able to both remove the internal stresses and also achieve minimum K_u. It may be necessary to first anneal in zero or longitudinal field to remove internal stresses and then anneal in transverse field for a short time at the same or a lower temperature to produce a low transverse K_u. Cooling rate may also influence K_u.

In some alloys, there may be changes in K_u during low-temperature aging. This would clearly be undesirable, and lack of severe aging effects should be another criterion for material selection. There may also be problems of reproducibility of K_u and other material parameters from sample to sample. The equations presented suggest that some of these potential problems could be controlled in device applications with the use of applied stresses to adjust or tune the effective anisotropy ($K_u - \frac{3}{2}\lambda_s\sigma$) of the sample.

We have considered the simple case of uniform H and/or σ directed exactly perpendicular to the induced anisotropy K_u. This yields the maximum magnetomechanical

coupling.[2]) The treatment can easily be extended to different relative orientations of H, σ, and K_u, but the equations become more complex. Bending or twisting stresses can be considered, and here the non-uniform σ also decreases the overall magnetomechanical coupling. Nevertheless, geometries producing bending or twisting will be advantageous in some device applications. In some applications, choice of material and operating conditions will be governed not by maximum magnetomechanical sensitivity, but by maximum ranges of linear response [13].

The magnetization process in the domain geometry assumed is pure rotation (Fig. 1b), with no contribution from domain-wall motion. Thus eddy-current losses should approximate those calculated from classical theory, i.e. there should be no "anomalous" losses. Because of the thinness of the ribbons and the high resistivity of the amorphous alloys, these classical eddy-current losses should be very low, far lower than those of conventional magnetostrictive materials. Another advantage of amorphous materials in magnetomechanical applications is their high mechanical strength.

4. Summary

A simplified model has been used to demonstrate why amorphous metals can exhibit outstanding magnetomechanical properties. Although high values of λ_s, M_s, and E_M are needed, a low value of K_u is of primary importance. The need for a low and homogeneous K_u should guide the selection of alloy composition and annealing conditions for optimum properties.

Acknowledgements

We acknowledge helpful discussions with A. E. Clark, H. T. Savage, and M. L. Spano, who independently developed a similar analysis in [5].

References

[1] C. MODZELEWSKI, H. T. SAVAGE, L. T. KABACOFF, and A. E. CLARK, IEEE Trans. Magnetics 17, 2837 (1981).
[2] M. A. MITCHELL, J. R. CULLEN, R. ABBUNDI, A. E. CLARK, and H. T. SAVAGE, J. appl. Phys. 50, 1627 (1979).
[3] M. BROUHA and J. VAN DER BORST, J. appl. Phys. 50, 7594 (1979).
[4] K. I. ARAI and N. TSUYA, Sci. Rep. Res. Inst. Tôhoku Univ., Suppl. A28, 247 (1980).
[5] M. L. SPANO, K. B. HATHAWAY, and H. T. SAVAGE, J. appl. Phys. 53, March 1982.
[6] J. D. LIVINGSTON, phys. stat. sol. (a) 56, 637 (1979).
[7] C. M. VAN DER BURGT, Philips Res. Rep. 8, 91 (1953).
[8] C. H. SHERMAN, IEEE Trans. Sonics Ultrasonics 22, 281 (1975).
[9] R. W. TIMME and S. W. MEEKS, J. Physique 40, Colloq. C5, 280 (1979).
[10] F. E. LUBORSKY and J. L. WALTER, IEEE Trans. Magnetics 13, 953 (1977).
[11] H. FUJIMORI, H. MORITA, Y. OBI, and S. OHTA, in: Amorphous Magnetism, Vol. 2, Ed. R. A. LEVY and R. HASEGAWA, Plenum Press, New York 1977 (p. 393).
[12] W. CHAMBRON and A. CHAMBEROD, Solid State Commun. 35, 61 (1980).
[13] I. J. GARSHELIS, IEEE IECI Conf. Proc. 76 CH1 117-1 IECI, 99 (1976).

(Received December 18, 1981)

[2]) The results would have been similar if the magnetic easy axis had been normal to the ribbon plane rather than widthwise. However, such an easy axis requires surface closure domains with in-plane magnetization [6], and magnetomechanical effects would be somewhat reduced unless there was also in-plane anisotropy to assure a widthwise magnetization direction for these closure domains.

APPENDIX B

Domain studies on amorphous ribbons with transverse or oblique magnetic anisotropy

J. D. Livingston, W. G. Morris, and F. E. Luborsky

General Electric Corporate Research and Development, Schenectady, New York 12301

SEM techniques are used to study domain structures in amorphous ribbons with transverse or oblique magnetic anisotropy. Domain widths are much finer than in ribbons with longitudinal anisotropy, and vary with ribbon dimensions and anisotropy constant. The effects of applied magnetic fields and applied stresses are also discussed.

PACS numbers: 75.60.Ch. 75.50.Kj

INTRODUCTION

In amorphous alloy ribbons, the easy axis of induced magnetic anisotropy can be varied by varying the orientation of the magnetic field applied during annealing. For 60-Hz transformer applications, a longitudinal easy axis has normally been induced. However, recent studies [1,2] have shown that an oblique or transverse easy axis produces lower ac losses because of (a) domain refinement and (b) an increasing component of rotation in the magnetization process (thus decreasing the component associated with domain-wall motion). This reduction of eddy-current losses is particularly important for high-frequency applications, and samples with transverse anisotropy tested at 50 kHz have been shown to approach classically-calculated power losses, i.e., with virtually no "anomalous" losses associated with wall motion [3]. Transverse magnetic anisotropy also produces maximum magnetomechanical coupling, and is therefore of interest for transducer and sensor applications.

Domain observations are important for understanding of magnetic and magnetomechanical properties, but most prior studies have been on as-cast or longitudinally-annealed ribbons. We report here domain structures in ribbons with oblique or transverse anisotropy, including the effects of ribbon dimensions, induced anisotropy constants, applied magnetic fields and applied stresses.

EXPERIMENTAL

Transverse-anisotropy ribbons of two different widths (0.16 cm and 1.27 cm) of each of two different alloys were received from the Naval Surface Weapons Center. The ribbons of Allied 2605 CO ($Fe_{67}Co_{18}B_{14}Si_1$) averaged 31 μm in thickness and the ribbons of Allied 2605 SC ($Fe_{81}B_{13.5}Si_{3.5}C_2$) averaged 19 μm in thickness, as measured by metallographic sectioning. Transverse anisotropy had been produced by annealing in a large (>1 kOe) magnetic field parallel to the ribbon width. The 2605 CO ribbons had been annealed for 10 minutes at 367°C, the 2605 SC ribbons for 10 minutes at about 380°C.

Also studied were samples of $Fe_{81}B_{15}Si_3C_1$, 1.27 cm wide and 20 μm thick, produced at General Electric and annealed for 2 hours at 343°C to produce oblique or transverse magnetic anisotropies [1]. Samples about 10 cm long were mounted in the sample stage employed in our previous studies [4]. Designed for insertion in a JEOL 200 kV SEM, this stage allows in-situ application of tensile stresses and dc and ac magnetic fields to the sample.

Transverse-annealed ribbons were mostly studied in a new sample stage which allows both rotation and tilting of the sample to achieve optimum domain contrast. Ribbons 4 cm long were generally rotated so that the tilt axis was parallel to the ribbon width (and initial magnetization direction). Domain observations were made on the air surfaces of the ribbons since the surface features, which also produce SEM contrast, are less severe on these surfaces.

RESULTS

Magnetic domain structures in the transverse-annealed 2605 CO ribbons are shown in Fig. 1. Average

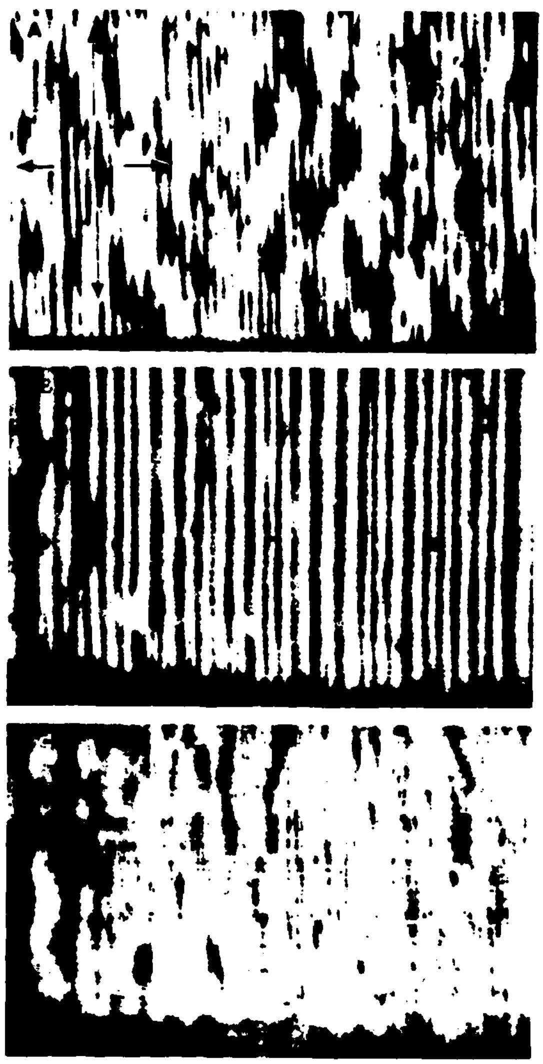

Fig. 1 Transverse-annealed 2605 CO ribbons. (a) Narrow ribbon after 200 Hz demagnetization. (b) Wide ribbon after 200 Hz demagnetization. (c) Same with applied longitudinal dc field of approximately 10 Oe. In these and subsequent figures, longitudinal axis of ribbon is horizontal and arrows indicate 1 mm. In above figures, ribbon edge visible at bottom.

domain widths after demagnetization with 200 Hz longitudinal fields were 45 μm in the narrow ribbon (Fig. 1a) and 70 μm in the wide ribbon (Fig. 1b). Further domain refinement occurs along the ribbon edge through the formation of spike domains, especially in the wide ribbon.

Application of a dc longitudinal magnetic field does not alter the transverse orientation of the magnetic domains, but does decrease the domain contrast and produces further domain refinement (Fig. 1c). Removal of the dc field leaves a domain structure that is 10-20% finer than that of the ac-demagnetized state. Domains were also observed after application and removal of a dc field of 6 kOe in the transverse direction, i.e., parallel to the domain width and magnetic easy axis. Domain widths were found to be similar to those following 200 Hz demagnetization in longitudinal fields (Figs. 1a, b).

The domain structure of the narrow 2605 SC ribbon after this transverse field treatment is shown in Fig. 2a. The domains are wider and wavier than those in the 2605 CO ribbon, and there is considerable curvature and splitting of the magnetic domains along the ribbon edge. Most of the observations reported above for the 2605 CO alloy were qualitatively similar for the 2605 SC. The average domain width after demagnetization in 200 Hz longitudinal fields was higher in the wide ribbon than in the narrow ribbon (150 μm vs. 120 μm). Application of a dc longitudinal field reduced domain contrast and produced domain refinement. After removal of this field, domains were finer than after 200 Hz demagnetization. However, regardless of field history, domains were always coarser and wavier in 2605 SC than in 2605 CO.

One unusual observation was a very marked curvature of the domains near one edge of the wide 2605 SC ribbon (Fig. 2b). This edge had been mechanically cut, and extensive shear bands were visible along the edge by optical microscopy. Edges of the narrow ribbon had also been cut, but apparently residual stresses were less severe.

Domains in the transverse-annealed GE alloy were similar to those in 2605 SC. After demagnetization in 200 Hz longitudinal fields (Fig. 3), the average domain width was 180 μm. As shown in Ref. 1, domains in oblique-anisotropy ribbons of this alloy were coarser, intermediate between the above widths and the 1.4 mm widths of longitudinal-anisotropy ribbon. Application of a longitudinal tensile stress to these ribbons produced domain rotation towards the longitudinal direction (Fig. 4). For the oblique-anisotropy ribbons, domain rotation with increasing stress was gradual, and the stress required to align the domains was higher for higher initial angles of inclination. However, domains in the transverse-annealed ribbon were found to rotate from transverse to longitudinal more abruptly with increasing stress.

DISCUSSION

Domains in the 2605 CO ribbons were found to be consistently straighter and finer than those in the other ribbons. We believe that both these observations stem from the higher induced anisotropy constant K of the 2605 CO alloy. Spano et al. [5] determined K = 38 J/m^3 for these 2605 SC ribbons. From comparison of measured anisotropy fields [1,5,6], we estimate K for the GE alloy to be about twice this value, and K for 2605 CO to be about an *order of* magnitude greater still.

The higher anisotropy of 2605 CO ties the magnetization more rigidly to the transverse direction than in the low-anisotropy 2605 SC and GE alloys, in which edge demagnetizing fields and residual or applied stresses as low as 1 MPa can significantly deflect domains. Such deviations in magnetization direction will cause departure from magnetic and magnetomechanical properties calculated assuming perfect transverse magnetization [5,7].

Domain widths in demagnetized transverse-anisotropy ribbons appear to be governed primarily by equilibrium considerations. The energy associated with domain walls favors coarse domains, but the magnetostatic energy associated with transverse demagnetizing fields favors fine domains. In low-anisotropy materials, the anisotropy constant K affects both terms. The domain-wall energy per unit area, γ, increases as $K^{1/2}$. However, the magnetostatic energy can be strongly reduced by deviations of the magnetization direction near the sample edge, the so-called μ*-effect. This effect depends on μ,* the susceptibility to magnetization rotation, which varies as K^{-1}. According to the theory of Kaczer [8], equilibrium domain width varies as $(\gamma\mu^*)^{1/3}$, and hence as $K^{-1/6}$. Thus, the much higher K of 2605 CO will lead

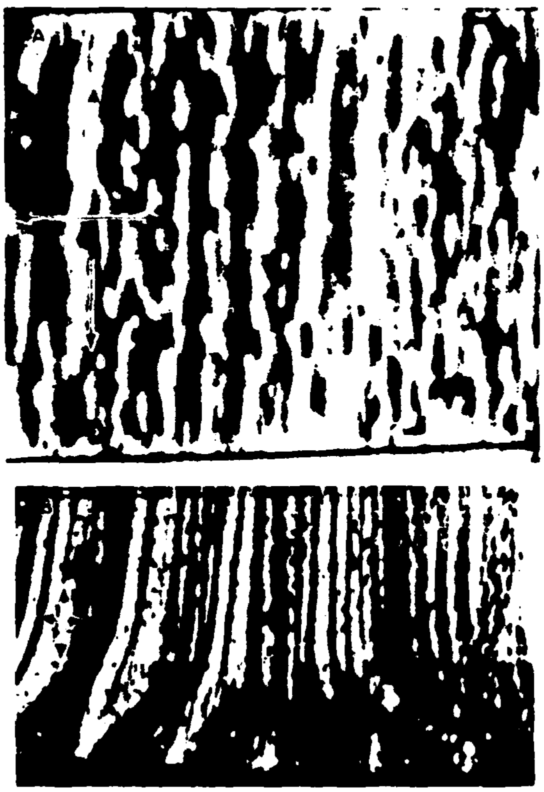

Fig. 2 Transverse-annealed 2605 SC ribbons. (a) Narrow ribbon after dc demagnetization in transverse field. Both edges of ribbon visible. (b) Wide ribbon after 200 Hz demagnetization, with domain curvature indicating residual stresses along cut edge, which is visible at bottom.

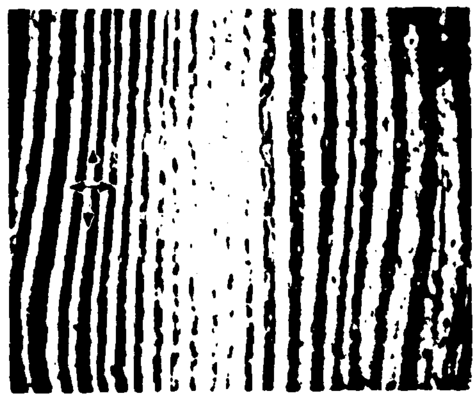

Fig. 3 Transverse-annealed GE Fe-B-Si-C ribbon after 200 Hz demagnetization. Domain curvature probably caused by small unintentional applied stresses.

to finer domains. The greater thickness of the 2605 CO ribbons undoubtedly also contributes, since this increases the transverse demagnetizing factor.

For longitudinal-anisotropy ribbons, 200 Hz demagnetization produced much finer domains than dc demagnetization [4]. This was clearly not an equilibrium effect, and resulted from the need for more 180° walls to keep up with the more rapid magnetization changes required under ac conditions. The same argument does not hold for transverse-anisotropy ribbons, since magnetization in longitudinal fields occurs primarily by rotation rather than wall motion. We observed in fact a slight inverse effect, i.e., finer domains after dc demagnetization than after ac demagnetization. We believe the latter domain widths are closer to equilibrium, the widths after dc demagnetization being a non-equilibrium remnant of the domain refinement observed under applied longitudinal field (Fig. 1c). The loss of domain contrast seen in this figure results from magnetization rotation towards the field direction, since it is the differing components of transverse magnetization that produce the contrast. The refinement of transverse domains by longitudinal field is reminiscent of the refinement of longitudinal domains by transverse field reported earlier [9]. Domain refinement by hard-axis magnetization has been observed also in crystalline materials [10,11], and may be associated with a transition from Bloch to Néel walls [11].

The domain rotation produced by applied tensile stress (Fig. 4) can be understood in terms of the superposition of the anneal-induced anisotropy at angle ϕ_o to the ribbon axis and a stress-induced anisotropy $K_\sigma = 3\lambda_s\sigma/2$ along the ribbon axis, where σ is the applied stress and λ_s is the saturation magnetization. Salzmann and Hubert [12] have shown how the variation of domain angle with stress can be used to calculate K/λ_s. Using their equation, the rotation observed in Fig. 4 can be used to yield $K/\lambda_s \sim 3$ MPa. Estimating $\lambda_s \sim 30 \times 10^{-6}$ yields $K \sim 90$ J/m^3, close to that estimated earlier for this alloy from magnetic data. Their equation also shows that as ϕ_o approaches 90°, domain rotation with increasing stress becomes more abrupt, as observed experimentally. In their idealized model assuming both anisotropies to be first-order uniaxial anisotropies, for ideal transverse anisotropy ($\phi_o = 90°$), the magnetic easy axis will change abruptly from transverse to longitudinal at $K_\sigma = K$. In reality, inhomogeneities and higher-order anisotropy terms will make the transition more gradual.

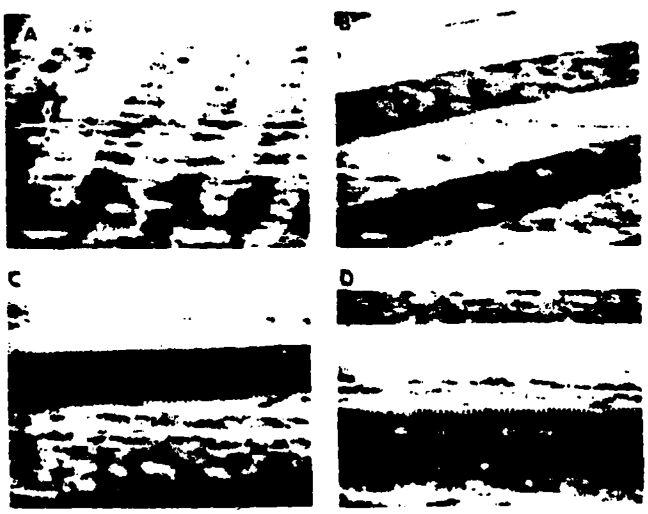

Fig. 4 Oblique-annealed GE Fe-B-Si-C ribbon showing rotation of domains by longitudinal tensile stress of (a) 0 MPa, (b) 3 MPa, (c) 7 MPa, (d) 14 MPa. Serrated image of some walls results from small applied ac field [4].

SUMMARY

1) Domains in transverse-anisotropy ribbons are much finer than in longitudinal-anisotropy ribbons because of the transverse demagnetizing factor. Domains are finer in narrow ribbons than in wide ribbons.

2) Domains in a high-anisotropy alloy (2605 CO) are straighter than in the lower-anisotropy 2605 SC and GE alloys, in which domain curvature from residual or applied stresses and local demagnetizing fields can be severe.

3) Domains are finer in the 2605 CO ribbons than in the other ribbons, partly because the higher K decreases the μ-effect on magnetostatic energy, and partly because of greater thickness.

4) Application of a dc longitudinal field to transverse-anisotropy ribbons decreases domain contrast and produces domain refinement. Some of this refinement is retained on removal of the field, leading to slightly finer domains after dc demagnetization than after ac demagnetization.

5) Application of longitudinal tensile stresses to ribbons with transverse or oblique anisotropy produces domain rotation, which can be used to determine K. Domain rotation is more abrupt for transverse anisotropy than for oblique anisotropy.

ACKNOWLEDGEMENTS

We are grateful to A.E. Clark, H.T. Savage and M.L. Spano of the Naval Surface Weapons Center for providing samples and for discussion. This work was supported in part by ONR.

REFERENCES

1. F.E. Luborsky and J.D. Livingston, IEEE Trans. Magn. MAG-18, 908 (1982).
2. H. Fujimori, H. Yoshimoto, and H. Morita, IEEE Trans. Magn. MAG-16, 1227 (1980).
3. R. Boll and H. Warlimont, IEEE Trans. Magn. MAG-17, 3053 (1981).
4. J.D. Livingston and W.G. Morris, IEEE Trans. Magn. MAG-17, 2624 (1981).
5. M.L. Spano, K.B. Hathaway and H.T. Savage, J. Appl. Phys. 53, 2667 (1982).
6. C. Modzelewski, H.T. Savage, L.T. Kabacoff and A.E. Clark, IEEE Trans. Magn. MAG-17, 2837 (1981).
7. J.D. Livingston, Phys. Stat. Sol. (a) 70, 591 (1982).
8. J. Kaczer, Sov. Phys. JETP 19, 1204 (1964).
9. R.F. Krause and F.E. Werner, IEEE Trans. Magn. MAG-17, 2686 (1981).
10. L.F. Bates and C.D. Mee, Proc. Phys. Soc., A65, 129 (1952).
11. R. Gemperle and M. Zeleny, Phys. Stat. Sol. 6, 839 (1964).
12. P. Salzmann and A. Hubert, J. Magn. Magn. Mater. 24, 168 (1981).

APPENDIX C

EFFECTS OF ANISOTROPY ON DOMAIN STRUCTURES IN AMORPHOUS RIBBONS

J. D. Livingston and W. G. Morris
General Electric Research & Development Center, Schenectady, NY 12301

T. Jagielinski[a)]
Department of Materials Science & Engineering, University of Pennsylvania, Philadelphia, PA 19104

Introduction

Although domain widths in amorphous ribbons with longitudinal magnetic anisotropy are determined primarily by magnetic history, domain widths in transverse-anisotropy ribbons are determined primarily by energetic considerations.[1] Equilibrium domain widths are determined by a balance between domain-wall energy and the magnetostatic energy associated with transverse demagnetizing fields. Earlier work on several Fe-rich amorphous alloys[1] indicated an influence of anisotropy constant, but a quantitative relationship was not established. A convenient alloy to study the effects of anisotropy constant is $Co_{70.3}Fe_{4.7}Si_{15}B_{10}$, since the kinetics of the development and reorientation of induced anisotropy are known in detail for this zero-magnetostriction alloy.[2-4]

In the present work, 1 mm-wide ribbons of this alloy were annealed in transverse field at various temperatures and times to produce transverse anisotropy constants varying from 140 to 1950 ergs/cc. Ribbons with lower anisotropy were produced by double anneals inducing a gradual reorientation from longitudinal to transverse anisotropy. Magnetic domain structures were studied by scanning electron microscopy (SEM) to determine the effects of varying anisotropy on domain widths, morphology, and behavior under applied magnetic fields.

Results

Despite the modest saturation magnetization of this alloy (~ 8000 gauss), the SEM produced good domain contrast, as seen in Fig. 1. The average domain width of transverse-anisotropy ribbons in a standard ac-demagnetized state was found to decrease with increasing anisotropy constant K as $K^{-1/6}$. This result is inconsistent with theoretical predictions of the original open-flux domain model of Kittel, but is consistent with the theories of Kaczer[5] and Hubert[6] that incorporate the μ^*-effect, i.e., the deflection of the magnetization vector from the easy direction near the ribbon edge by the demagnetizing fields. This μ^*-effect decreases the magnetostatic energy of transverse demagnetizing fields, and becomes increasingly important at low anisotropies, thereby increasing the equilibrium domain width. It also reveals itself by increasing domain curvature near the ribbon edge as anisotropy decreases. This departure from perfect transverse magnetization will influence the susceptibility (and, in alloys with non-zero magnetostriction, the magnetomechanical coupling) of transverse-anisotropy ribbons. The refinement of transverse domains by applied longitudinal

[a)]On leave from the Institute of Physics, Polish Academy of Sciences, 02-668 Warsaw, Poland.

Fig. 1. Magnetic domain structure in $Co_{70.3}Fe_{4.7}Si_{15}B_{10}$ ribbon annealed to produce a transverse anisotropy constant of 1950 ergs/cc. Arrows indicate 1 mm.

fields reported earlier for Fe-rich alloy ribbons[1] is not observed in these ribbons, suggesting that magnetostriction may have been a major cause of the refinement observed earlier.

In double-annealed ribbons with very low transverse anisotropy, domain structures were coarse, irregular, and more dependent on magnetic history than in the ribbons with higher transverse anisotropy. After ac demagnetization, domain structures were observed to coarsen with time over periods of many minutes. Domain widths approach the ribbon width, and the theories of Kaczer and Hubert are no longer valid.

Ribbons with longitudinal anisotropy, including as-cast ribbon, contained only one or two domain walls in the demagnetized state. Dynamics of the reversal process (nucleation and growth of reverse domains) could be studied in detail by varying the applied magnetic field during production of the scanning image.

This work was supported in part by ONR.

References

1. J. D. Livingston, W. G. Morris and F. E. Luborsky, Paper FP-10, Intermag-3M Conference, Montreal (1982).
2. K-Y Ho, P. J. Flanders and C. D. Graham, Jr., J. Appl. Phys. 53, 2279 (1982).
3. K-Y Ho, Papers FP-7 and 8, Intermag-3M Conference, Montreal (1982).
4. T. Jagielinski, Paper FP-19, Intermag-3M Conference, Montreal (1982).
5. J. Kaczer, Sov. Phys. JETP 19, 1204 (1964).
6. A. Hubert, Phys. Stat. Sol. (a) 24, 669 (1967).

4-8

DTI